Modeling of Turbulence and Transition

Tsan-Hsing Shih

1. Motivation and Objective

The first objective is to evaluate current two-equation and second order closure turbulence models using available direct numerical simulations and experiments, and to identify the models which represent the state of the art in turbulence modeling.

The second objective is to study the near-wall behavior of turbulence, and to develop reliable models for an engineering calculation of turbulence and transition.

The third objective is to develop a two-scale model for compressible turbulence.

2. Work Accomplished

2.1 Evaluation of two-equation models (N.J. Lang and T.-H. Shih[1])

Twelve two-equation models including $k - \epsilon$, $k - \tau$, $k - \omega$ and $q - \omega$ models, have been evaluated using a common flow solver code (GENMIX) for wall bounded turbulent flows. For each model, calculations were carried out for two-dimensional, fully developed channel and flat plate boundary layer flows. These flows are appealing for model testing because they are simple and self-similar, yet demonstrate important features of wall bounded turbulent shear flows. In addition, we can compare these calculations with Direct Numerical Simulations (DNS). A list of the models which were tested are shown in the table below:

Ch	Chien[2] 1982	$k - \epsilon$
Sh	Shih[3] 1991	$k - \epsilon$
LB	Lam and Bremhorst[4] 1981	$k - \epsilon$
NH	Nagano and Hishida[5] 1987	$k - \epsilon$
NT	Nagano and Tagawa[6] 1990	$k - \epsilon$
LS	Launder and Sharma[7] 1974	$k - \epsilon$
JL	Jones and Launder[8] 1973	$k - \epsilon$
MK	Myong and Kasagi[9] 1988	$k - \epsilon$
YS	Yang and Shih[10] 1991	$k - \epsilon$
WI1	Wilcox[11] 1984	$k - \omega$
WI2	Wilcox[12] 1991	$k - \omega$
SAA	Speziale, Abid and Anderson[13] 1990	$k - \tau$
Co	Coakley[14] 1983	$q - \omega$

Two dimensional channel flow calculations were made at $Re_\tau = 180$ and $Re_\tau = 395$. These cases were compared with DNS data of Kim et al[15]. Calculations for the two-dimensional flat plate boundary layer flow at $Re_\theta = 1410$ were compared with DNS data of Spalart[16]. Some flat plate boundary layer comparisons were made

between the experimental data of Klebanoff[17] at $Re_\theta = 7700$ and solutions of the various models. The detailed results are reported in NASA TM 105237, 1991.

An important criterion for two-equation model comparisons is not only how well the model predicts mean velocity and shear stress, but also the turbulent kinetic energy and dissipation (or specific dissipation) rate. These predictions should provide appropriate turbulent velocity and length scales so that the model can be applied to more complex flows for which a simple mixing length model often fails. Some researchers maintain that it is not critical whether or not the turbulent kinetic energy and the turbulent length scale are predicted with great accuracy. However, one may imagine that a two-equation model making unreasonable turbulent velocity and length scale predictions would be very questionable when applied to more general flows. A model which accurately predicts the shear stress and mean velocity does not imply that it has correctly modeled the turbulent kinetic energy and length scale. In fact, if the turbulent kinetic energy is incorrect, then the length scale must also be incorrect to compensate for the error in the turbulent kinetic energy. For this case, two wrongs are making a right. This warrants some caution when computing flows for other geometries.

Comments on two-equation models:

It is clear that the JL, LS, WI1 and WI2 models underpredict the near wall turbulent kinetic energy compared to the other models.

The standard $k - \epsilon$ model has been proven to provide good results in the high Reynolds number range. It is therefore attractive for a near wall $k - \epsilon$ turbulence model to approach the standard $k - \epsilon$ model away from the wall. The LB, LS and YS models are the only $k - \epsilon$ models in this study which possess this characteristic.

Because boundary layer and channel flows are self-similar, the solutions should be independent of the initial conditions. However, some of the models (SAA, Co, and LB) have difficulty when the initial conditions contain large gradients. The Co Model is particularly dependent on the initial conditions. Even slight perturbations of the initial conditions will yield noticeably different solutions with this model.

JL, LS, WI1 and WI2 are the only models which do not contain y^+. Damping functions which contain y^+ are not desirable because y^+ is erroneous near flow separations and not well defined near complicated geometries. Unfortunately, these are the same models which poorly predict the near wall turbulent quantities.

The Wilcox models (WI1 and WI2) suffer from a numerically awkward boundary condition for ω at the wall:

$$\omega \to \frac{6\nu}{C_2 y^2} \text{ as } y^+ \to 0$$

We cannot define ω at $y^+ = 0$. We have tried two ways to approximate ω as y^+ approaches 0. First, we chose a large number for ω_{wall} and, second, we used an asymptotic $\omega_{wall} = \frac{6\nu}{C_2 y^2}$. Test cases showed that the solution does not converge as $\omega_{wall} \to \infty$ when $y^+ \to 0$ for either model. In addition, both Wilcox models underpredict the turbulent kinetic energy peak value for both boundary layer and channel flows.

model the new unknowns T_{ij}, Π_{ij} and ε_{ij}. At the level of the second order closure, these new unknowns are usually modeled with algebraic equations in terms of the second moments and the mean quantities (with the exception of the trace $\varepsilon_{kk} = 2\varepsilon$, which is modeled with a transport equation).

In a general turbulent shear flow with moderate inhomogeneity, the turbulent diffusion terms in the second moment equations are usually smaller than the other terms. However, the pressure-strain rate and dissipation rate tensors are always among the leading terms. Therefore, the performance of modeled equations largely depends on the models of pressure-strain rate tensor and dissipation rate tensor.

In this study, we only concentrate on the models of the pressure-strain rate tensor and the dissipation rate tensor for the velocity field: $\Pi_{ij} - \varepsilon_{ij}$, which are modeled as

$$\Pi_{ij} - \varepsilon_{ij} = \Pi_{ij}^{(1)} + \Pi_{ij}^{(2)} - \frac{2}{3}\varepsilon\delta_{ij}$$

where $\Pi_{ij}^{(1)}$, $\Pi_{ij}^{(2)}$ are respectively referred to as the rapid term and the return-to-isotropy term.

Models for the rapid term $\Pi_{ij}^{(1)}$

Launder, Reece and Rodi (LRR):[18]

$$\frac{\Pi_{ij}^{(1)}}{2q^2} = 0.2S_{ij} + \frac{9C_2 + 6}{22}(b_{ik}S_{jk} + b_{jk}S_{ik} - \frac{2}{3}\delta_{ij}b_{kl}S_{kl})$$
$$+ \frac{10 - 7C_2}{22}(b_{ik}\Omega_{jk} + b_{jk}\Omega_{ik}) \qquad (2.2.1)$$

where $C_2 = 0.4$, and

$$b_{ij} = \frac{\overline{u_i u_j}}{q^2} - \frac{1}{3}\delta_{ij},$$

$$S_{ij} = \frac{1}{2}(U_{i,j} + U_{j,i}),$$

$$\Omega_{ij} = \frac{1}{2}(U_{i,j} - U_{j,i})$$

This model is linear in the Reynolds-stress. It contains only one model constant C_2. This model satisfies the conventional model constraints[34]. It is the most general form at the level of linear dependence on the Reynolds-stress. However, as Lumley[24] pointed out, this model may violate realizability as the turbulence approaches a two-component state.

Speziale, Sarkar and Gatski (SSG):[19]

$$\frac{\Pi_{ij}^{(1)}}{2q^2} = \frac{0.8 - C_3^{**}}{4}S_{ij} - \frac{C_1^* P}{2q^2}b_{ij}$$
$$+ \frac{C_4}{4}(b_{ik}S_{jk} + b_{jk}S_{ik} - \frac{2}{3}\delta_{ij}b_{kl}S_{kl})$$
$$+ \frac{C_5}{4}(b_{ik}\Omega_{jk} + b_{jk}\Omega_{ik}) \qquad (2.2.2)$$

where,

$$C_3^{**} = C_3^*(b_{ij}b_{ij})^{1/2}, \quad P = -\overline{u_iu_j}U_{i,j}$$
$$C_1^* = 1.8 \quad C_3^* = 1.3, \quad C_4 = 1.25, \quad C_5 = 0.4$$

This model is quasi-linear in the Reynolds-stress, because the coefficients in the first two terms are not constant, but depend on the invariant of the Reynolds-stress tensor and the production P. This model contains four model constants (C_1^*, C_3^*, C_4, C_5), therefore one may imagine that it will be difficult to correctly calibrate them. In addition, this model does not satisfy the normalization constraint which is one of the basic model constraints[34]. If we impose this constraint, then the four coefficients will reduce to only one, and this model will reduce to the LRR model. Finally, like the LRR model, the SSG model may also violate realizability.

Fu, Launder and Tselepidakis (FLT):[20]

$$
\begin{aligned}
\frac{\Pi_{ij}^{(1)}}{2q^2} = {} & 0.2S_{ij} + 0.3(b_{ik}S_{jk} + b_{jk}S_{ik} - \frac{2}{3}\delta_{ij}b_{kl}S_{kl}) \\
& + \frac{1.3}{3}(b_{ik}\Omega_{jk} + b_{jk}\Omega_{ik}) \\
& + 0.2(b_{il}^2 S_{jl} + b_{jl}^2 S_{il} - 2b_{kj}b_{li}S_{kl} - 3b_{ij}b_{kl}S_{kl}) \\
& + 0.2(b_{il}^2 \Omega_{jl} + b_{jl}^2 \Omega_{il}) \\
& + r[4b_{nn}^2(b_{ik}\Omega_{jk} + b_{jk}\Omega_{ik}) \\
& + 12b_{mi}b_{nj}(b_{mk}\Omega_{nk} + b_{nk}\Omega_{mk})]
\end{aligned}
\tag{2.2.3}
$$

where $r = 0.7$, $b_{ij}^2 = b_{ik}b_{kj}$.

This model is cubic in the Reynolds-stress. The final form selected contains one model constant. This model only satisfies a part of the realizability condition, corresponding to a two-component state of turbulence. However, when a scalar field is involved, this model cannot satisfy Schwarz' inequality between velocity and temperature. This part of realizability is sometimes called joint realizability.

Shih and Lumley (SL):[21]

$$
\begin{aligned}
\frac{\Pi_{ij}^{(1)}}{2q^2} = {} & 0.2S_{ij} + 3\alpha_5(b_{ik}S_{jk} + b_{jk}S_{ik} - \frac{2}{3}\delta_{ij}b_{kl}S_{kl}) \\
& + \frac{1}{3}(2 - 7\alpha_5)(b_{ik}\Omega_{jk} + b_{jk}\Omega_{ik}) \\
& + 0.2(b_{il}^2 S_{jl} + b_{jl}^2 S_{il} - 2b_{kj}b_{li}S_{kl} - 3b_{ij}b_{kl}S_{kl}) \\
& + 0.2(b_{il}^2 \Omega_{jl} + b_{jl}^2 \Omega_{il})
\end{aligned}
\tag{2.2.4}
$$

where,

$$\alpha_5 = \frac{1}{10}(1 + 0.8F^{1/2}), \quad F = 1 + 9b_{ij}b_{jk}b_{ki} - \frac{9}{2}b_{ij}b_{ij}$$

This model is quasi-quadratic in the Reynolds-stress, because the model coefficient α_5 is a function of the invariants of the Reynolds-stress tensor. We emphasize that

this model is obtained from a more general form of the expression than the FLT, and satisfies both the two component condition and Schwarz' inequality between the velocity and scalar fields. In addition, the final form is simpler than the model of FLT.

Shih and Mansour (SM):[22]

$$
\frac{\Pi^{(1)}_{ij}}{2\overline{q^2}} = 0.2S_{ij} + 3\alpha_5(b_{ik}S_{jk} + b_{jk}S_{ik} - \frac{2}{3}\delta_{ij}b_{kl}S_{kl})
$$
$$
+ \frac{1}{3}(2 - 7\alpha_5)(b_{ik}\Omega_{jk} + b_{jk}\Omega_{ik}) \qquad (2.2.5)
$$
$$
+ 0.2(b^2_{il}S_{jl} + b^2_{jl}S_{il} - 2b_{kj}b_{li}S_{kl} - 3b_{ij}b_{kl}S_{kl})
$$
$$
+ 0.2(b^2_{il}\Omega_{jl} + b^2_{jl}\Omega_{il})
$$

where, $\alpha_5 = \frac{1}{10}\{1 + 3.5[1 - (1 - F)^{1/4}]\}$.

This model has the same form as the SL model. It was derived in a different way and contains a different model coefficient α_5 which was calibrated from one of the DNS data (Rogers[30]). This model, like the SL model, fully satisfies realizability conditions.

Models for the return-to-isotropy term $\Pi^{(2)}_{ij}$

Rotta:[23]

$$
\Pi^{(2)}_{ij} = -\varepsilon C b_{ij} \qquad (2.2.6)
$$

where, $C = 3.0$.

This model is linear in the Reynolds stress, and contains one model constant. It was widely used and adopted in the LRR model. We notice that this model will not allow the turbulence to reach a two-component state, because when any turbulent component reduces to $\overline{q^2}/9$, the model Eq.(2.2.6) will force it to grow.

Lumley:[24]

$$
\Pi^{(2)}_{ij} = -\varepsilon[\beta b_{ij} + \gamma(b^2_{ij} + 2II\delta_{ij}/3)] \qquad (2.2.7)
$$

where, $\gamma = 0$ and

$$
\beta = 2 + \frac{F}{9}\exp(-7.77/\sqrt{Re})\{72/\sqrt{Re} + 80.1\ln[1 + 62.4(-II + 2.3III)]\}
$$
$$
Re = \frac{\overline{q^2}^2}{9\varepsilon\nu}
$$

This model is quasi-linear in the Reynolds stress, because γ is set to zero, and β is a function of the invariants of Reynolds stress tensor. This model is simple, and satisfies realizability.

Sarkar and Speziale (SS):[25]

$$
\Pi^{(2)}_{ij} = -\varepsilon[C_1 b_{ij} - 3(C_1 - 2)(b^2_{ij} - \frac{1}{3}b^2_{kk}\delta_{ij})] \qquad (2.2.8)
$$

where $C_1 = 3.4$.

This is a quadratic model in the Reynolds-stress tensor. It satisfies what is called the weak realizability condition. Like the Rotta model Eq.(2.2.8), this model will not produce unphysical results. However, it will not allow the turbulence to approach a two-component state, which could occur in some situations, for example, in near-wall turbulence.

Haworth and Pope (HP):[26]

$$\Pi_{ij}^{(2)} = -\varepsilon\{C_1 b_{ij} - C_2[\frac{1}{3}b_{ij} + b_{ij}^2 - b_{kk}^2(b_{ij} + \delta_{ij}/3)]\} \tag{2.2.9}$$

where $C_1 = 8.3$, $C_2 = 14.8$.

Eq.(2.2.9) is a slow part of the Haworth and Pope's model for the situations with no mean velocity gradient. This model, like the SS model, will not produce unphysical results; however, it will also not allow the turbulence to approach a two-component state.

Choi and Lumley (CL):[27]

If $III \geq 0$,

$$\Pi_{ij}^{(2)} = -\varepsilon[\beta b_{ij} + \gamma(b_{ij}^2 + 2II\delta_{ij}/3)] \tag{2.2.10.1}$$

where,

$$\beta = 2 + \frac{\rho^* F^{1/2}}{1 + G\chi^2}$$

$$\gamma = \frac{\rho^* F^{1/2}}{1 + G\chi^2}\frac{G}{\xi}$$

$$\xi = (III/2)^{1/3}, \quad \eta = (-II/3)^{1/2}$$

$$\chi = \frac{\xi}{\eta}, \quad G = -\chi^4 + 0.8\chi^6$$

$$\rho^* = \exp[-9.29/Re^{1/2}]\{(\frac{7.69}{Re^{1/2}} + \frac{73.7}{Re}) - [296 - 16.2(\chi + 1)^4]II\}$$

$$Re = \frac{\overline{q^2}^2}{9\varepsilon\nu}, \quad II = -b_{ij}b_{ij}/2, \quad III = b_{ij}b_{jk}b_{ki}/3$$

If $III < 0$,

$$\Pi_{ij}^{(2)} = Eq.(28) \tag{2.2.10.2}$$

The model coefficients in Eq.(2.2.10.1) were obtained using their comprehensive measurements of turbulence relaxing from axisymmetric expansion. Both Eq.(2.2.10.1) and Eq.(2.2.10.2) satisfy realizability; however, Eq.(2.2.10.1) is valid only for $III \geq 0$, because ξ is not defined when $III < 0$.

Craft and Launder (C&L):[28]

$$\Pi_{ij}^{(2)} = -C_1\varepsilon[2b_{ij} + 4C_1'(b_{ij}^2 - b_{kk}^2\delta_{ij}/3)] - 2\varepsilon b_{ij} \tag{2.2.11}$$

where,

$$C_1 = 3.1(A_2 A)^{1/2}, \quad C_1' = 1.2$$

$$A_2 = 4\, b_{ij} b_{ji}, \quad A_3 = 8\, b_{ij} b_{jk} b_{ki}, \quad A = 1 - \frac{9}{8}(A_2 - A_3)$$

This model is tensorially quadratic in the Reynolds stress, and satisfies realizability.

Yamamoto and Arakawa (YA):[29]

$$\Pi_{ij}^{(2)} = -\varepsilon[\alpha_1 b_{ij} + \alpha_2(b_{ij}^2 - b_{kk}^2 \delta_{ij}/3)] \tag{2.2.12}$$

where,

$$\alpha_1 = 2 + p\, F\, [q\,(b_{kk}^2)^r + |b_{kk}^3|^s sign(b_{kk}^3)]$$

$$\alpha_2 = 3\,(\alpha_1 - 2)$$

$$p = -12, \quad q = -0.65, \quad r = 0.4, \quad s = 0.45$$

$$F = 1 - \frac{9}{2} b_{kk}^2 + 9\, b_{kk}^3$$

The YA model tried to fit situations with both positive and negative b_{kk}^3. It also meets the requirement of realizability.

Shih and Mansour (S&M):[22]

$$\Pi_{ij}^{(2)} = -\varepsilon\{(2.0 + C_f F^\xi)b_{ij} + \gamma[b_{ij}^2 + (1/3 + 2II)b_{ij} + \frac{2}{3}II\delta_{ij}]\} \tag{2.2.13}$$

where,

$$C_f = (1/9)\exp(-7.77/\sqrt{Re})\{72/\sqrt{Re} + 80.1\ln[1 + 62.4(-II + 2.3III)]\}$$

$$\gamma = \gamma_0(1 - F^\eta), \quad Re = \frac{\overline{q^2}^2}{9\varepsilon\nu}$$

$$F = 1 + 9II + 3III$$

$$II = -\frac{1}{2}b_{ij}b_{ij}, \quad III = \frac{1}{3}b_{ij}b_{jk}b_{ki}$$

$$\xi = 17/20, \quad \eta = 1/20, \quad \gamma_0 = -2$$

This model matches the data of Comte-Bellot and Corrsin[21] and meets the requirement that there will be no return to isotropy in the zero Reynolds number limit. This model also satisfies realizability.

Concluding remarks

We notice that the Reynolds number in all these simulations is low and therefore may not represent real turbulence in nature. However, the model terms concerned here are mainly pressure related correlations. The fluctuating pressure is not directly related to the viscosity, hence the pressure related correlation terms may not be directly affected by the Reynolds number, especially the rapid term. The return-to-isotropy term, which includes the deviatoric part of the dissipation rate

tensor may have some dependence on the Reynolds number. According to the above consideration, we think that direct comparisons with low-Reynolds DNS data are legitimate, although we should keep in mind the possible low-Reynolds number effect of the DNS data.

We have directly compared five rapid models with fifteen DNS flows: four of Rogers et al.'s[30] shear flows, eleven of Lee et al.'s[31] irrotational strain flows (axisymmetric contraction, axisymmetric expansion and plane strain). Comparing the performance of the LRR and SSG models, which are tensorially linear in the Reynolds stress, we conclude that the SSG model gives very little improvement over the LRR model. In fact in many cases, it is worse than the LRR model. The reason is not very clear. However, we notice that the SSG model does not satisfy the normalization condition which may be a cause for its poor behavior. If we impose this constraint on the SSG model, then it will exactly reduce to the LRR model. In fact it can be shown that the most general form of the rapid model, which is tensorially linear in the Reynolds stress, is the LRR model. Therefore, in general, the treatment used in the SSG model would hardly give any improvement over the LRR model. A natural way to improve the model is to use a more general nonlinear form and more general model constraints. A typical example is the SL[21] model. It starts with the most general form, using full realizability constraints together with the other conventional constraints[34]. The result is a well behaved model. Indeed, from the direct comparisons with the DNS data, the SL[21] model and its variation form of SM[22] model give the best performance in most of the cases. As to the FLT[20] model, it is also a nonlinear model. It starts with a tensorially cubic dependance on the Reynolds stress with *constant* coefficients (in general, these coefficients should not be restricted to constants). In addition, the two-component conditions of turbulence have been imposed. However, the FLT model ignores Schwarz' inequality. Its final form contains two undetermined model constants, but one of them is set to zero. The performance of the FLT model, from the direct comparisons with the DNS data, is better overall than the linear models, but does not compare with the performance of the SL and SM models. So from these direct comparisons of the rapid models, we conclude that the SL[21] model and its variation form SM[22] are clearly the best. Having said this we notice that, as Reynolds[33] pointed out, any of these rapid models will not show any effect of rotation on the invariants (II, III) of the anisotropy tensor b_{ij}. This is clearly a theoretical deficiency of the current rapid models. A further investigation is needed to find out how serious this deficiency will be in practice.

We have directly compared eight return-to-isotropy models with thirty four DNS flows: four shear flows and thirty relaxation flows from axisymmetric contraction, axisymmetric expansion and plane strain. As was discussed earlier, all the return-to-isotropy models are variations of Eq.(2.2.7) derived by Lumley[24]. Therefore the differences in the models are due to the different choices of the model coefficients. Two linear models are due to Rotta[23] and Lumley[24] (which is quasi-linear in b_{ij}). Lumley's model satisfies realizability, matches the data of Comte-Bellot

and Corrsin[32] and the limit of the final period of decaying turbulence. It performs perfectly when $III < 0$. It also compares well with the DNS data in which $III \geq 0$. Rotta's model does not compare with the performance of Lumley's model. In fact, the nonlinear models of SS, YA, HP and C&L also do not compare with the performance of Lumley's model. Apparently the model coefficients chosen in these models are not appropriate. The CL[27] model is designed for flows with $III \geq 0$ and is based on their experiments on relaxing turbulence. It does work better than Lumley's model when $III \geq 0$. Finally, the S&M[22] model is a nonlinear model; it works just like Lumley's model when $III < 0$. When $III \geq 0$, it shows an improvement over Lumley's model according to the DNS data. So from these direct comparisons of the return-to-isotropy models, we conclude that the combination of Lumley's model and Choi's model, that is the CL[27] model, will give the best performance. The S&M[22] model seems as good as the CL model according to these comparisons. Having said this, we notice that the existing return-to-isotropy models do not follow the relaxation flows from expansion and plane strain very well. Therefore there is still a need to further investigate and improve the return-to-isotropy models.

For detailed comparison in each flow see the reference[34].

2.3 Near-wall behavior of turbulence

The near-wall behavior of turbulence is re-examined in a way different from that proposed by Hanjalic and Launder[35] and followers[36,37,38,3]. It is shown that at a certain distance from the wall, all energetic large eddies will reduce to *Kolmogorov* eddies (the smallest eddies in turbulence). All the important wall parameters, such as friction velocity, viscous length scale, and mean strain rate at the wall, are characterized by *Kolmogorov* microscales. According to this *Kolmogorov* behavior of near-wall turbulence, the turbulence quantities, such as turbulent kinetic energy, dissipation rate, etc. at the location where the large eddies become "*Kolmogorov*" eddies, can be estimated by using both direct numerical simulation (DNS) data and asymptotic analysis of near-wall turbulence. This information will provide useful boundary conditions for the turbulent transport equations. As an example, the concept is incorporated in the standard k-ε model which is then applied to channel and boundary layer flows. Using appropriate boundary conditions (based on *Kolmogorov* behavior of near-wall turbulence), there is no need for any wall-modification to the k-ε equations (including model constants). Results compare very well with the DNS and experimental data.

Here we only list the results from this study, for the detail see NASA TM 105663.

Model equation and boundary condition

The K-ε equations for incompressible flows can be in general modeled as:

$$\frac{DK}{Dt} = [(\nu + \frac{\nu_T}{\sigma_k})K_{,i}]_{,i} + \nu_T U_{i,j}(U_{i,j} + U_{j,i}) - \varepsilon \tag{2.3.1}$$

$$\frac{D\varepsilon}{Dt} = [(\nu + \frac{\nu_T}{\sigma_\varepsilon})\varepsilon_{,i}]_{,i} + C_1 f_1 \nu_T U_{i,j}(U_{i,j} + U_{j,i})\frac{\varepsilon}{K}$$

$$- C_2 f_2 \frac{\varepsilon^2}{K} + \nu\nu_T U_{i,jk}U_{i,jk} \tag{2.3.2}$$

$$C_1 = 1.44, \quad C_2 = 1.92$$

$$f_1 = 1, \quad f_2 = 1 - 0.22 \exp\left(-\frac{R_t^2}{36}\right), \quad R_t = \frac{K^2}{\nu\varepsilon} \tag{2.3.3}$$

$$\sigma_k = 1, \quad \sigma_\varepsilon = 1.3$$

These equations are used only for the flow field outside of the turbulence limit point y_η, where K_η is non-zero. Therefore, Eq.(2.3.2) will not have singularity problems and will not need any near-wall modifications like other K-ε models do.[2,8]
Eddy viscosity:

$$\nu_T = C_\mu f_\mu \frac{K^2}{\varepsilon} \tag{2.3.4}$$

where,

$$C_\mu = 0.09$$

$$f_\mu = [1 - \exp(a_1 R_k + a_3 R_k^3 + a_5 R_k^5)]^{\frac{1}{2}}$$

$$a_1 = -1.5 * 10^{-4} \quad a_3 = -1.0 * 10^{-9} \quad a_5 = -5.0 * 10^{-10} \tag{2.3.5}$$

$$R_k = \frac{K^{1/2} y}{\nu}$$

Boundary conditions: at $y_\eta = 6\nu/u_\tau$,

$$\varepsilon_\eta = 0.251 \frac{u_\tau^4}{\nu} \tag{2.3.6}$$

$$K_\eta = 0.250 u_\tau^2 \tag{2.3.7}$$

In practical applications, $R_{e\tau}$ and $R_{e\infty}$ are large numbers, hence y_η/L (L is the length scale of a flow field) is usually very small. Therefore, as an approximation we may let $y_\eta/L = 0$, but ε_η and K_η must be given by Eqs.(2.3.6) and (2.3.7) respectively. These equations have been applied to the calculations of channel and boundary layer flows.

Comparison of models

To compare the present model with the DNS data and other models (e.g. Jones and Launder[8], and Chien[2]), we have made calculations on two channel flows[15,40] and two boundary layer flows[16,17]. In the present model, all the model constants are the same as used in the standard K-ε model[39]. Therefore the present model will also be suitable for flows away from the wall. The other two models used here for comparison do not have this property. Results are shown in figures 1 – 4. In figure 1 and figure 2, three models are compared with two DNS data for channel flows: one with $R_{e\tau} = 180$, the other with $R_{e\tau} = 395$. The profiles of mean velocity, Reynolds stress, turbulent kinetic energy and its dissipation rate are plotted in these figures. The present model is significantly better than the other two models. Figure 3 shows the similar comparison for a turbulent boundary with $R_{e\theta} = 1410$. The agreement between the present model and DNS data is excellent. Figure 4 shows

the results compared with Klebanoff[17] and other boundary layer experiments. The skin friction from DNS data[16] is also shown in this figure. The results of present model are more consistent with the DNS data than the experiments.

It is also worthwhile to emphasize that the present model equations with the standard model coefficients have the simplest form among all two-equation models. Hence, we expect that they will have less numerical stiffness in complex turbulent flows.

2.4 Modeling of transition (Z. Yang and T.-H. Shih)

A model of intermittancy based on the shape factor is added to a two-equation k-ε model for prediction of boundary layer transition with a free stream turbulence. The detailed model and calculations are give by Yang in this year's Research Briefs.

2.5 Modeling of compressible turbulence (W.W. Liou and T.H. Shih)

A two-scale model is proposed based on Hanjalic-Launder's multiple-scale concept for compressible turbulence, in which a distinct scale created by the compressibility is modeled separately by considering the effects of pressure-dilatation and dissipation dilatation on large-scale energy transfer rate. The detailed model is given by Liou in this year's Research Briefs.

2.6 Direct numerical simulation of compressible flows (A. Hsu and T.-H. Shih)

In order to have a better understanding of the effect of compressibility on turbulence, especially the effect of the formation of eddy-shocklets on turbulence, a direct numerical simulation of compressible homogeneous shear turbulent flows is been performing. The data of all turbulence statistics are very useful for turbulence modeling. The detailed simulation is given by Hsu in this year's Research Briefs.

3. Future Plans

Development of second order closure models: pay special attention to the effects of inhomogeneity, non-local property, frame-rotation, compressibility, near-wall behavior in the buffer and log-layers.

4. References

1 Lang, H.J. and Shih, T.-H., "A critical comparison of two-equation turbulence models," NASA TM 105237 (1991).

2 Chien, K.-Y., "Predictions of Channel and Boundary-Layer Flows with a Low-Reynolds-Number Turbulence Model," AIAA Journal, 20, 33-38, (1982).

3 Shih, T. -H., An Improved $k - \varepsilon$ Model for Near-Wall Turbulence and Comparison with Direct Numerical Simulation," NASA TM-103221, August (1990).

4 Lam, C. K. G., and Bremhorst, K., "A Modified Form of the k-ε Model for Predicting Wall Turbulence," ASME Transaction, Journal of Fluids Engineering, 103, September (1981).

5 Nagano, Y. and Hishida, M., "Improved Form of the k-ε Model for Wall Turbulent Shear Flows," ASME Transaction, Journal of Fluids Engineering, 109, June (1987).

6   Nagano, Y., and Tagawa, M., "An Improved k-ϵ Model for Boundary Layer Flows," ASME Transaction, Journal of Fluids Engineering, **112**, March (1990).

7   Launder, B. E. and Sharma, B. I., "Application of the Energy-Dissipation Model of Turbulence to the Calculation of a Flow near a Spinning Disk," Letters in Heat and Mass Transfer, **1**, 131-138 (1974).

8   Jones, W. P. and Launder, B. E., "The Calculation of Low-Reynolds Number Phenomena with a Two-Equation Model of Turbulence," International Journal of Heat and Mass Transfer, **16**, 1119-1130 (1973).

9   Myong, H. K. and Kasagi, N., "A new Proposal for a k-ϵ Turbulence Model and its Evaluation." JSME Transaction, **54**, 3003-3009 and 3512-3520 (1988).

10 Yang, Z. and Shih, T. -H., "A $k - \epsilon$ Modeling of Near Wall Turbulence," Proceedings of 4th International Symposium on Computational Fluid Dynamics, UC Davis (1991).

11 Wilcox, D. C., "A Complete Model fo Turbulence Revisited, " AIAA Paper no. 84- 0176, Reno, Nevada (1984).

12 Wilcox, D. C., "Progress in Hypersonic Turbulence Modeling," AIAA Paper no.91-1785, Honolulu, HI (1991).

13 Speziale, C. G., Abid, R. and Anderson, E. C., "A Critical Evaluation of Two-Equation Models for Near Wall Turbulence," AIAA Paper no. 90-1481, Seattle, WA (1990).

14 Coakley, T. J., "Turbulence Modeling Methods for the Compressible Navier-Stokes Equations," AIAA Paper no. 83-1693, Danvers, Massachusetts (1983).

15 Kim, J., Moin, P. and Moser, R., "Turbulent Statistics in fully Developed Channel Flow at Low Reynolds Number," Journal of Fluid Mechanics, **177**, 133-166 (1987).

16 Spalart, P. R., "Direct Simulation of a Turbulent Boundary Layer up to $Re_\theta = 1410$," Journal of Fluid Mechanics, **187**, 61-98 (1988).

17 Klebanoff, P. S., "Characteristics of Turbulence in a Boundary Layer with Zero Pressure Gradient," NACA-TN-3178 (1954).

18 Launder, B.E., Reece, G.J., & Rodi, W. , " Progress in the development of a Reynolds-stress turbulence closure," J. Fluid Mech. (1975), **68**, 537-566 (1975).

19 Speziale, C.G., Sarkar, S. and Gatski, T.B., "Modeling the pressure-strain correlation of turbulence: an invariant dynamical systems approach," *J. Fluid Mech.*, **227**, 245-272 (1991).

20 Fu, S., Launder, B.E. and Tselepidakis, D.P., "Accommodating the effects of high strain rates in modeling the pressure-strain correlation. *UMIST Mech. Engng Dept Rep.* TFD/87/5, 1987.

21 Shih, T.-H. & Lumley, J.L., " Modeling of pressure correlation terms in Reynolds stress and scalar flux equations." Rep. FDA-85-3, *Sibley School of Mech. & Aero. Engrg.*, Cornell University (1985).

22 Shih, T.-H. and Mansour, N.N., "Reynolds Stress Modeling of Homogeneous Turbulence and Comparison with Numerical Simulations," *Center for Turbulence Research* Proceedings of the Summer Program (1987).

23 Rotta, J.C., Z. Phys. **129**, 547 (1951).

24 Lumley, J.L., "Computational modeling of turbulent flows," *Adv. Appl. Mech.* **18**, 123 (1978).

25 Sarkar, S. and Speziale, C.G., "A simple nonlinear model for the return to isotropy in turbulence," Phys. Fluids, A2 (1), January, (1990).

26 Haworth, D.C. and Pope, S.B., "A generalized Langevin model for turbulent flows," Phys. fluid **29** (2), February (1986).

27 Choi, K.S. and Lumley, J.L., *Proceedings of the IUTAM symposium, Kyoto, 1983, Turbulence and Chaotic phenomena in Fluids*, edited by T.Tatsumi (North-Holland, Amsterdam), p.267 (1984).

28 Craft, T.J. and Launder, B.E., "Computation of Impinging Flows Using Second-Moment Closure," Eighth Symposium on Turbulent Shear Flows, Technical University of Munich, September 9-11 (1991).

29 Yamamoto, M. and Arakawa, c., "Study on the pressure-strain term in Reynolds stress model," *Eighth Symposium on Turbulent Shear Flows*, Technical University of Munich, September, 9-11 (1991).

30 Rogers, M.M., Moin, P. & Reynolds, W.C., "The structure and modeling of the hydrodynamic and passive scalar fields in homogeneous turbulent shear flow," Dept. Mech. Engng. Rep. TF-24, Stanford University: Stanford California (1986).

31 Lee, M.J. & Reynolds, W.C., " Numerical experiments on structure of homogeneous turbulence," Dept. Mech. Engng. Rep. TF-24, Stanford University: Stanford California (1985).

32 Comte-Bellot, G. and Corrsin, S., " The use of a contraction to improve the isotropy of grid-generated turbulence," J. Fluid Mech. **25**, 657-682 (1966).

33 Reynolds, W.C.," Effect of Rotation on Homogeneous Turbulence," Tenth Australian Fluid Mechanics Conference, December 11-15 (1989).

34 Shih, T.-H. and Lumley, J.L., "A Critical Comparison of Second Order Closures with Direct Numerical Simulation of Homogeneous Turbulence," NSAS TM 105351 (1991).

35 Hanjalic, K. and Launder, B.E., "Contribution Towards a Reynolds-stress Closure for Low–Reynolds–Number Turbulence," J. Fluid Mech, **74**, 593–619 (1976).

36 Patel, V.C., Rodi, W. and Scheuerer, G., "Turbulence models for near–wall and low–Reynolds–number flows: A review," AIAA Journal, **23**, 1308–1319 (1985).

37 Mansour, N.N., Kim,J. and Moin. P., "Reynolds-Stress and Dissipation Rate Budgets in a Turbulent Channel Flow," J. Fluid Mech., **194**, 15–44 (1988).

38 Lai, Y.G. and So, R.M.C., "On near-wall turbulent flow modeling," J. Fluid Mech. **221**, 641-673 (1990).

39 Launder, B.E. and Spalding, D.B., "Computer Methods in Applied Mechanics and Engineering, **3**, 269 (1974).
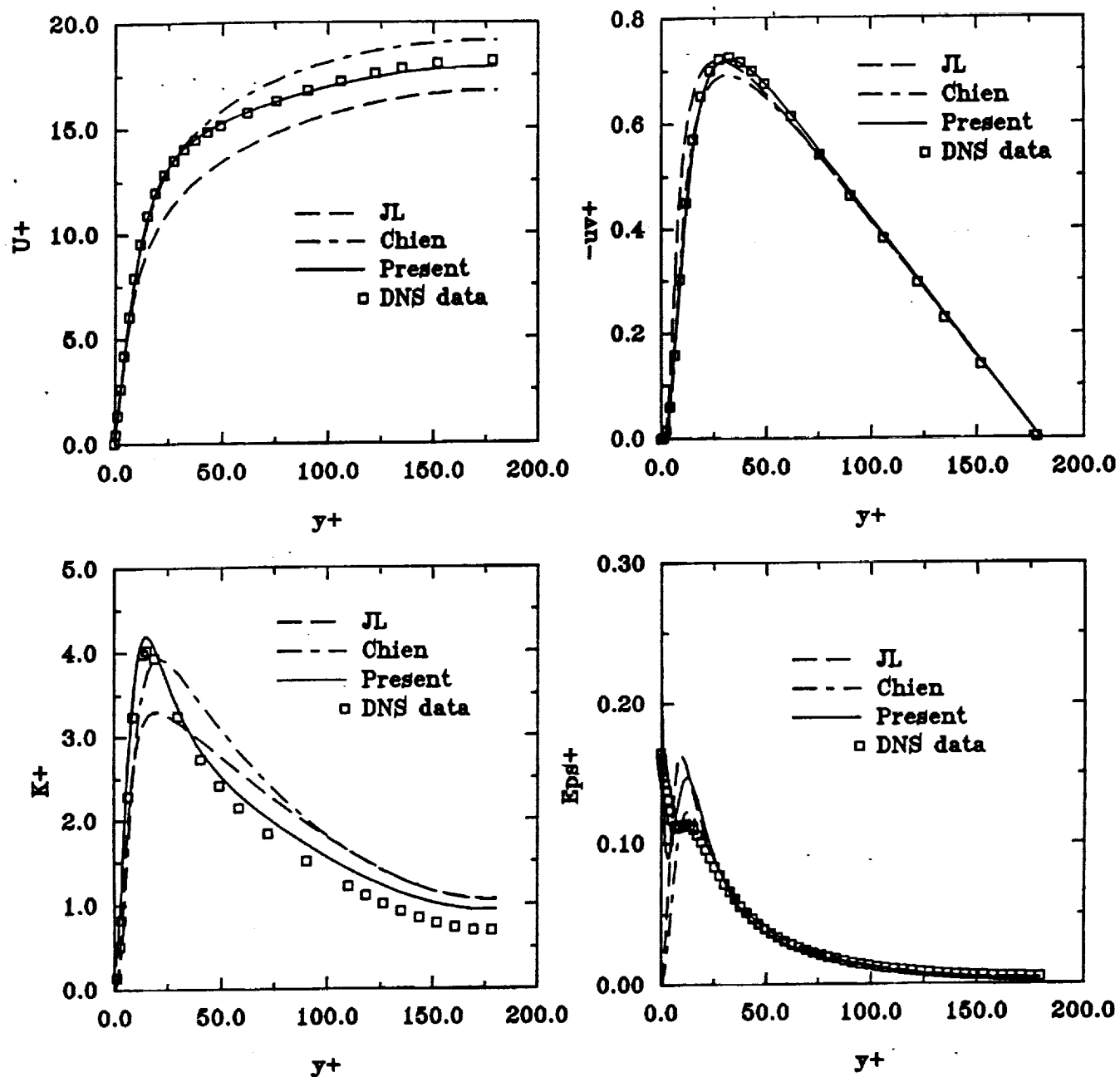
40 Kim, J., Personal communication, 1992.

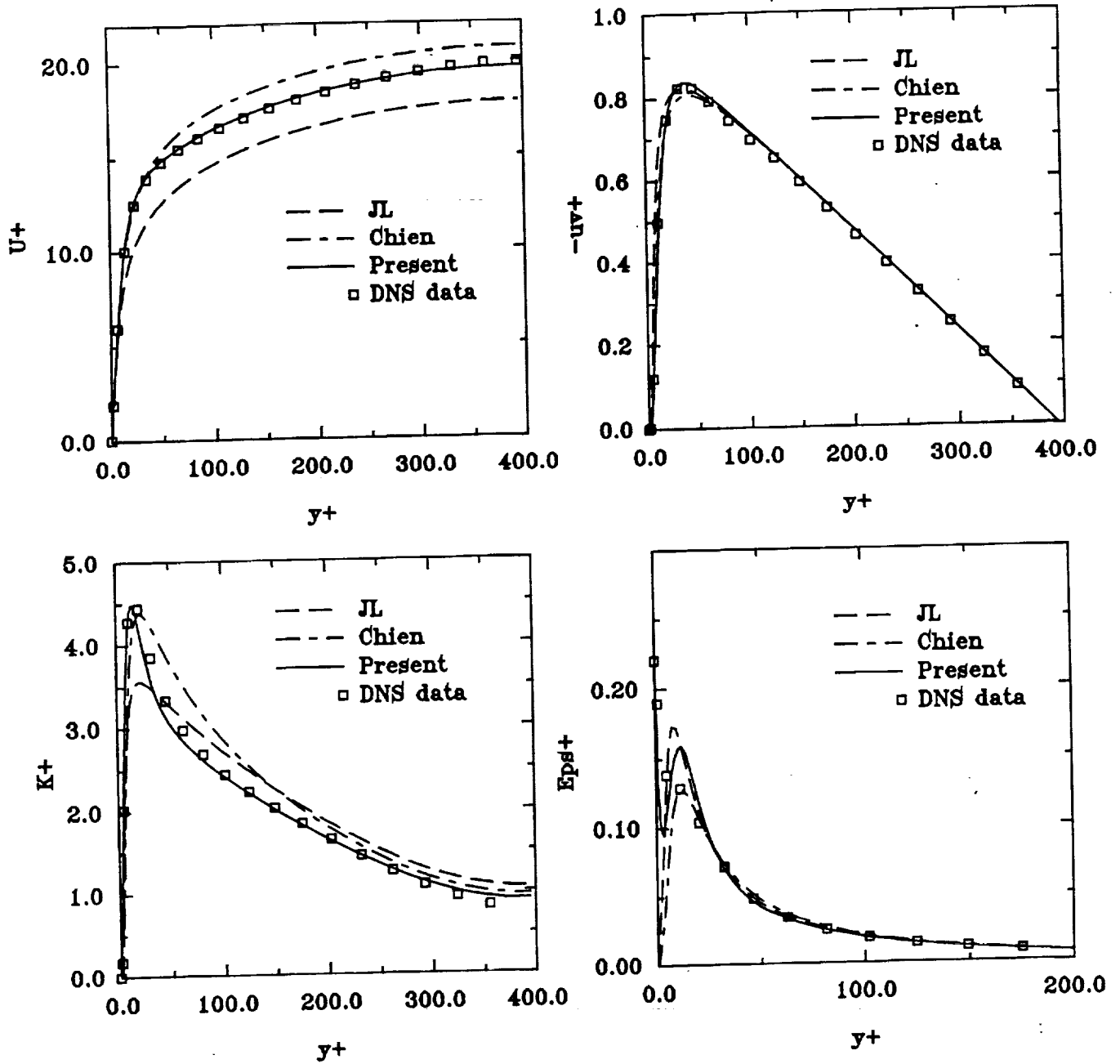Figure 1. Comparison of models with DNS of 2-D channel with $R_{e\tau} = 180$.

Figure 2. Comparison of models with DNS of 2-D channel with $R_{e\tau} = 395$.
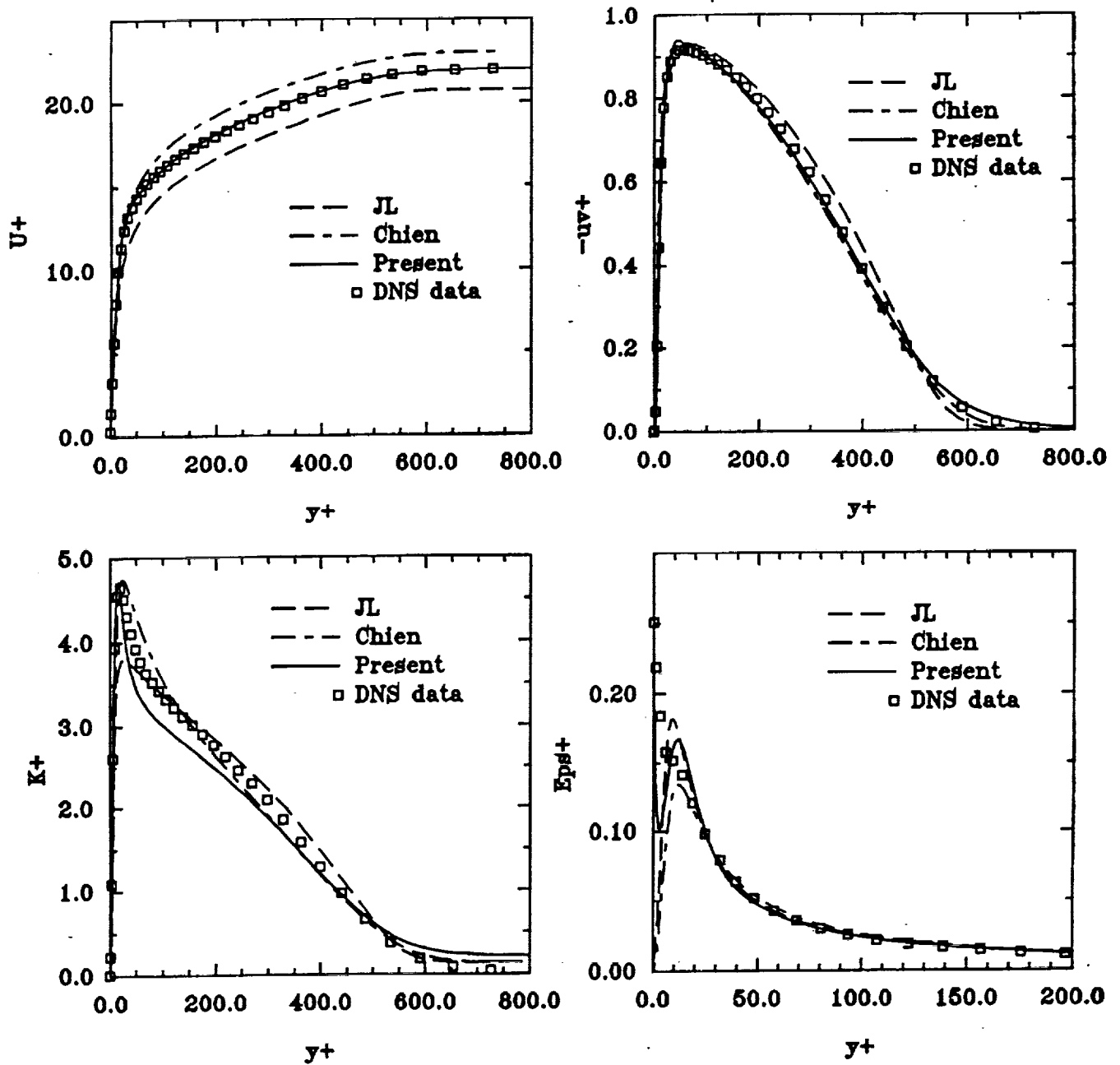
Figure 3. Comparison of models with DNS of 2-D boundary layer flow
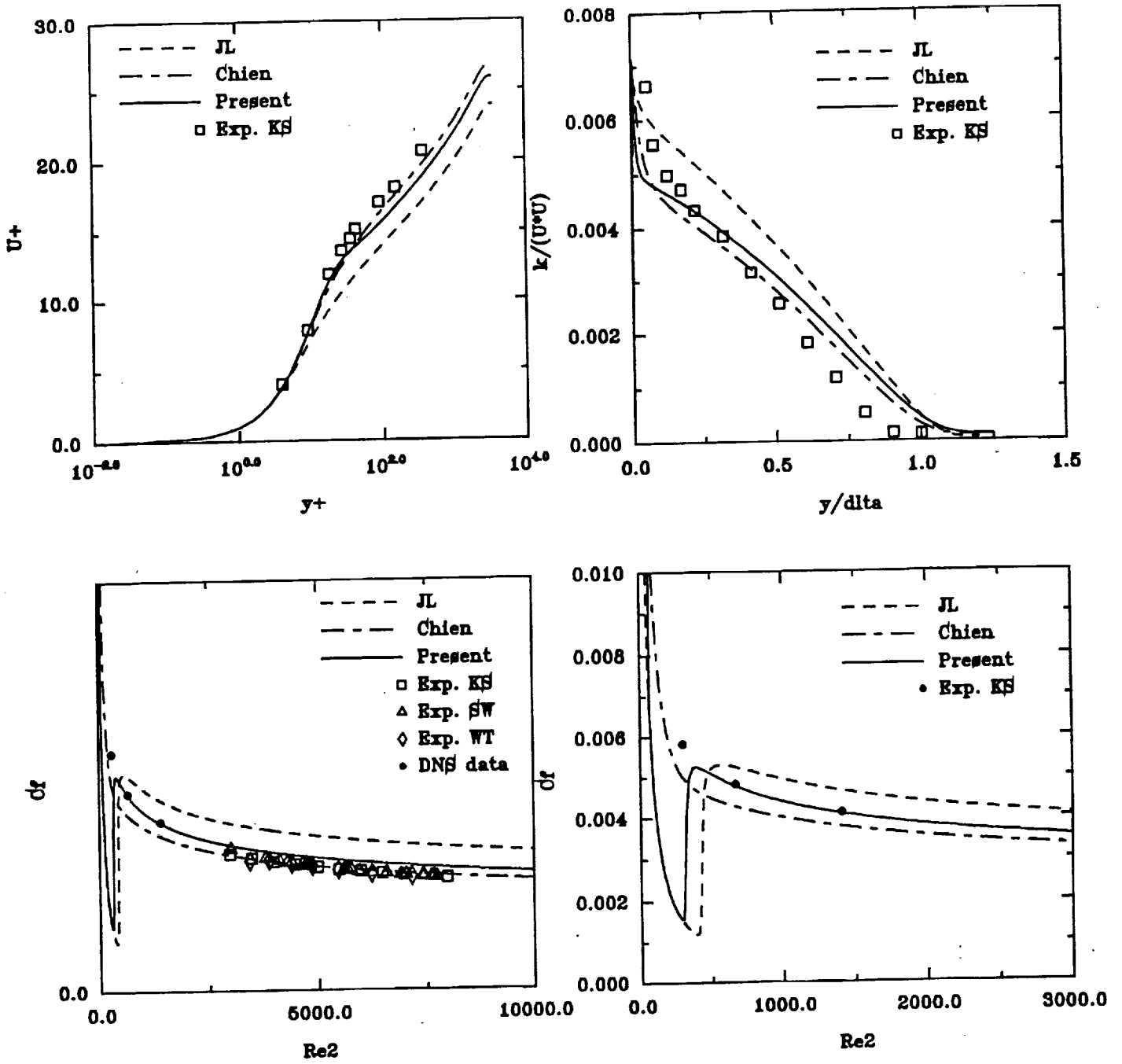with $R_{e\theta} = 1410$.

Figure 4. Comparison of models with the experiments of 2-D boundary layer flows (Klebanoff[13] and others).